

Lateral interactions between adsorbed molecules: Investigations of CO on Ru(001) using nonlinear surface vibrational spectroscopies

Minhaeng Cho*

Department of Chemistry and Center for Multidimensional Spectroscopy, Korea University, Seoul 136-701, Korea

Christian Hess

Fritz Haber Institut der Max Planck Gesellschaft, Faradayweg 4-6, 14195 Berlin, Germany

Mischa Bonn

Leiden Institute of Chemistry, P.O. Box 9502, 2300 RA Leiden, The Netherlands

(Received 12 December 2001; published 23 May 2002)

We present an experimental and theoretical investigation into the coupling of C-O stretch vibrations of CO molecules adsorbed on Ru(001). We employ surface infrared-visible (IR-VIS) (IV) and infrared-infrared-visible (IR-IR-VIS) (IIV) sum-frequency generation (SFG) (IV-SFG and IIV-SFG, respectively) to investigate the effects of the intermolecular coupling through the nonlinear optical response of the system. As a consequence of the increased intermolecular interaction with increasing coverage due to the closer proximity of CO molecules on the surface, we observe pronounced frequency shifts of the vibrational resonances. In addition, the intensity behavior in both the IV-SFG and IIV-SFG spectra exhibits a strong nonlinear dependence on the coverage. These observations can be reproduced by extending previous theories for the coverage-dependent linear optical response (used to explain IR reflectance absorption data) to the nonlinear optical response. Expressions are derived for the second- and third-order nonlinear susceptibilities in terms of molecular properties such as the polarizability, hyperpolarizability, and second hyperpolarizability. We obtain very good quantitative agreement between theory and experiment. The analysis indicates that the principal effect of the intermolecular coupling on the nonlinear optical response is through a local-field correction for the linear IR field.

DOI: 10.1103/PhysRevB.65.205423

PACS number(s): 68.35.Ja, 33.20.Ea, 33.40.+f, 42.65.-k

I. INTRODUCTION

Surface sum-frequency-generation (SFG) spectroscopies have been used extensively to study vibrational dynamics and properties of adsorbed molecules on surfaces as well as at interfaces.¹⁻⁶ These three-wave-mixing spectroscopies measure the lowest-order nonlinear optical response of adsorbed molecules, which contains important information on, e.g., the local chemical surroundings of molecules on surfaces and their orientation.⁷ In particular, the infrared-visible SFG (IV-SFG) as first proposed and demonstrated by Shen and co-workers^{2,3} has been used to investigate vibrational dephasing and physical and chemical processes of molecules adsorbed on a metal surface.¹⁻²³ It involves the interaction of adsorbed molecules with an infrared field (ω_{ir}) resonant with a molecular vibration, so that a temporal transient polarization is created by the IR-field-matter interaction. The vibrationally coherent state thus created is probed by detecting the sum-frequency field ($\omega_{\text{ir}} + \omega_{\text{vis}}$) radiated by the second-order polarization, after an interaction of the surface with a second, nonresonant visible pulse with frequency ω_{vis} . In the frequency domain, the width of the IV-SFG peak corresponds to the vibrational dephasing constant, whereas the decaying pattern of the time-resolved IV-SFG signal measurement can provide information on the vibrational dephasing rate in the time domain—note that the vibrational population relaxation rate and the pure dephasing rate can be measured by using an IR pump-IR/SFG probe^{13,14,19,24} scheme and IR/SFG photon-echo techniques,²⁰ respectively. If the adsorbed molecules

undergo a chemical transformation, one can use this method to investigate the real-time chemical reaction dynamics as well as underlying physical processes such as surface-phonon coupling with the adsorbed molecules.²⁵

Although highly successful, the IV-SFG method is limited by being a one-dimensional vibrational spectroscopy, since only one variable, either the infrared field frequency (in a frequency-domain measurement) or the delay time between the IR and visible pulses (in a time-domain measurement), is experimentally controlled. Recently, we presented a theoretical extension of IV-SFG to a two-dimensional vibrational spectroscopy involving two infrared fields and one visible field, where the sum frequency of the infrared fields with the visible field is generated, viz., infrared-infrared-visible SFG (IIV-SFG).^{26,27} Two IR fields create a two-dimensional transient grating in the optical sample, and the electronically off-resonant visible field is used to generate the third-order polarization, which radiates the IIV-SFG field. This technique is ideally suited to study coupling between vibrational modes at surfaces,²⁷ in analogy to two-dimensional vibrational spectroscopies in bulk media.²⁸⁻³⁸

Indeed, the recent experimental observation of IIV-SFG (Ref. 39) from the C-O stretch vibration of carbon monoxide on Ru(001) demonstrated that the IIV-SFG method can provide useful information on the vibrational coupling between neighboring CO molecules by comparing signals at different CO fractional coverages θ .³⁹ However, the experimental results were interpreted within the framework of localized vibrations, where the coupling between molecules

was treated as a perturbation. In reality, the CO stretching motions at high coverages are considerably delocalized due to the lateral interaction, mainly of a dipole-dipole nature.^{40,41} Furthermore, this interpretation was complicated due to the investigation at very high coverages [a comparison was made between signals for $\theta=0.33$ and 0.68 monolayers (ML)]. However, for $\theta>0.33$ ML, the intermolecular interaction is not very well defined as will be shown below.

Therefore, in this paper, we present experimental results of IV- and IIV-SFG under well-defined conditions of $0<\theta<0.33$ ML, and a theoretical framework for the interpretation of these signals as a function of the fractional coverage that explicitly includes the strong interaction between molecules at higher coverages. To this end, we shall first present a general theoretical description of the IV- and IIV-SFG processes (in Sec. II). The experimental method for the measurements of the IV- and IIV-SFG signals of incomplete monolayers of CO molecules on the Ru(001) surface is presented in Sec. III. In Sec. IV, the experimental findings are theoretically analyzed and the linear and nonlinear optical properties of the adsorbed CO molecules on Ru(001) are discussed. Finally, the main results will be summarized in Sec. VI.

II. GENERAL RELATIONSHIPS OF THE MOLECULAR POLARIZABILITY AND HYPERPOLARIZABILITIES WITH THE MACROSCOPIC LINEAR AND NONLINEAR SUSCEPTIBILITIES

In order to obtain relationships of the molecular polarizability and hyperpolarizabilities with the macroscopic linear and nonlinear susceptibilities, the local field $E_l(\mathbf{r},t)$, Maxwell field $E(\mathbf{r},t)$, and polarization $P(\mathbf{r},t)$ are first expanded in a discrete Fourier series, i.e., $E_l(\mathbf{r},t) = \sum_j [E_l(\mathbf{k}_j, \omega_j) \exp(i\mathbf{k}_j \cdot \mathbf{r} - i\omega_j t) + \text{c.c.}]$, etc. Here, the index j labels those modes relevant for the experiment. $P(\mathbf{r},t)$ is the polarization per unit volume at position \mathbf{r} . Since the magnitudes of the optical and IR wave vectors are usually small compared to the length scale of microscopic fluctuations, the system can be assumed to be homogeneous.

Then, the polarization can be written as a power series with respect to local fields, i.e.,

$$\begin{aligned}
 P(\mathbf{r},t) = & \rho_0 \sum_j \alpha(\omega_j) E_l(\mathbf{k}_j, \omega_j) \exp(i\mathbf{k}_j \cdot \mathbf{r} - i\omega_j t) \\
 & + \rho_0 \sum_{j \geq n} \beta(\omega_j, \omega_n) E_l(\mathbf{k}_j, \omega_j) E_l(\mathbf{k}_n, \omega_n) \\
 & \times \exp[i(\mathbf{k}_j + \mathbf{k}_n) \cdot \mathbf{r} - i(\omega_j + \omega_n)t] \\
 & + \rho_0 \sum_{j \geq n \geq m} \gamma(\omega_j, \omega_n, \omega_m) E_l(\mathbf{k}_j, \omega_j) E_l(\mathbf{k}_n, \omega_n) \\
 & \times E_l(\mathbf{k}_m, \omega_m) \exp[i(\mathbf{k}_j + \mathbf{k}_n + \mathbf{k}_m) \cdot \mathbf{r} \\
 & - i(\omega_j + \omega_n + \omega_m)t] + \dots
 \end{aligned} \quad (1)$$

The three terms in Eq. (1) denote the linear, and second- and third-order nonlinear contributions to the polarization. These

are proportional to the linear polarizability, first hyperpolarizability, and second hyperpolarizability of a single molecule, respectively, denoted as α , β , and γ . The number density is denoted as ρ_0 .

Although Eq. (1) is an exact expression for the polarization, one would like to express it in terms of a power series of the Maxwell field. Introducing the susceptibilities, we have

$$P(\mathbf{r},t) = P^{(1)}(\mathbf{r},t) + P^{(2)}(\mathbf{r},t) + P^{(3)}(\mathbf{r},t) + \dots, \quad (2)$$

where

$$\begin{aligned}
 P^{(1)}(\mathbf{r},t) = & \sum_j \chi^{(1)}(-\mathbf{k}_j, -\omega_j; \mathbf{k}_j, \omega_j) E(\mathbf{k}_j, \omega) \\
 & \times \exp(i\mathbf{k}_j \cdot \mathbf{r} - i\omega_j t),
 \end{aligned}$$

$$\begin{aligned}
 P^{(2)}(\mathbf{r},t) = & \sum_{j \geq n} \chi^{(2)}(-\mathbf{k}_j - \mathbf{k}_n, -\omega_j - \omega_n; \mathbf{k}_j, \omega_j, \mathbf{k}_n, \omega_n) \\
 & \times E(\mathbf{k}_j, \omega_j) E(\mathbf{k}_n, \omega_n) \exp[i(\mathbf{k}_j + \mathbf{k}_n) \cdot \mathbf{r} \\
 & - i(\omega_j + \omega_n)t],
 \end{aligned}$$

$$\begin{aligned}
 P^{(3)}(\mathbf{r},t) = & \sum_{j \geq n \geq m} \chi^{(3)}(-\mathbf{k}_j - \mathbf{k}_n - \mathbf{k}_m, -\omega_j - \omega_n \\
 & - \omega_m; \mathbf{k}_j, \omega_j, \mathbf{k}_n, \omega_n, \mathbf{k}_m, \omega_m) \\
 & \times E(\mathbf{k}_j, \omega_j) E(\mathbf{k}_n, \omega_n) E(\mathbf{k}_m, \omega_m) \\
 & \times \exp[i(\mathbf{k}_j + \mathbf{k}_n + \mathbf{k}_m) \cdot \mathbf{r} - i(\omega_j + \omega_n + \omega_m)t].
 \end{aligned} \quad (3)$$

Note that the linear and nonlinear susceptibilities are expansion coefficients of each term, when the polarization is expanded in terms of the Maxwell field.

Now, the remaining task is to express the susceptibilities in terms of microscopic susceptibilities, such as α , β , and γ . In the wave-vector space, the local field is related to the Maxwell field as

$$E_l(\mathbf{k},t) = E(\mathbf{k},t) - \frac{U(\mathbf{k})}{\rho_0} P(\mathbf{k},t). \quad (4)$$

Here the second term on the right-hand side of Eq. (4) represents the electrostatic field created by all other particles. U represents the dipole-dipole and dipole-image-dipole interactions, etc.⁴⁰⁻⁴³ Here, it should be emphasized that the polarization $P(\mathbf{k},t)$ is also dependent on the Maxwell field so that the problem should be solved in a self-consistent manner.

A. Linear susceptibility and definition of the local-field correction factor, $S(\mathbf{k},\omega)$

We will first consider the first-order polarization, by considering the first-order local field,

$$E_l^{(1)}(\mathbf{k},t) = E(\mathbf{k},t) - \frac{U(\mathbf{k})}{\rho_0} P^{(1)}(\mathbf{k},t). \quad (5)$$

From Eq. (1), the first-order polarization component $P^{(1)}(\mathbf{k}, \omega)$ can be rewritten as, after inserting Eqs. (5) into (1),

$$P^{(1)}(\mathbf{k}, \omega) = \rho_0 \alpha(\omega) \left\{ E(\mathbf{k}, \omega) - \frac{U(\mathbf{k})}{\rho_0} P^{(1)}(\mathbf{k}, \omega) \right\}. \quad (6)$$

Thus, we have

$$P^{(1)}(\mathbf{k}, \omega) = \frac{\rho_0 \alpha(\omega)}{1 + \alpha(\omega) U(\mathbf{k})} E(\mathbf{k}, \omega). \quad (7)$$

From the definitions of the linear susceptibility in Eq. (3), i.e.,

$$P^{(1)}(\mathbf{k}, \omega) = \chi^{(1)}(-\mathbf{k}, -\omega; \mathbf{k}, \omega) E(\mathbf{k}, \omega) \quad (8)$$

and comparing Eqs. (7) with (8), the linear susceptibility is found to be

$$\chi^{(1)}(-\mathbf{k}, -\omega; \mathbf{k}, \omega) = \frac{\rho_0 \alpha(\omega)}{1 + \alpha(\omega) U(\mathbf{k})}. \quad (9)$$

The local-field correction term $S(\mathbf{k}, \omega)$ is defined as

$$S(\mathbf{k}, \omega) \equiv \frac{1}{1 + \alpha(\omega) U(\mathbf{k})}. \quad (10)$$

Thus, in the first-order approximation, the local and Maxwell fields are related to each other as

$$E_l^{(1)}(\mathbf{k}, \omega) = S(\mathbf{k}, \omega) E(\mathbf{k}, \omega). \quad (11)$$

B. Second-order nonlinear susceptibility

We next consider the second-order nonlinear susceptibility. If the second- and higher-order polarization components are taken into account, the local field can be expressed as

$$E_l(\mathbf{k}, \omega) = S(\mathbf{k}, \omega) E(\mathbf{k}, \omega) - \frac{U(\mathbf{k})}{\rho_0} \{ P^{(2)}(\mathbf{k}, \omega) + P^{(3)}(\mathbf{k}, \omega) + \dots \}. \quad (12)$$

Inserting Eqs. (12) into (1) and collecting the second-order terms only, we find

$$P^{(2)}(\mathbf{k}, \omega) = \rho_0 \alpha(\omega) \left\{ - \frac{U(\mathbf{k})}{\rho_0} P^{(2)}(\mathbf{k}, \omega) \right\} + \rho_0 \beta(\omega_1, \omega_2) \times \{ S(\mathbf{k}_1, \omega_1) E(\mathbf{k}_1, \omega_1) \} \{ S(\mathbf{k}_2, \omega_2) E(\mathbf{k}_2, \omega_2) \}. \quad (13)$$

From the above equation, the second-order polarization component can be expressed as

$$P^{(2)}(\mathbf{k}, \omega) = \frac{\rho_0 \beta(\omega_1, \omega_2) S(\mathbf{k}_1, \omega_1) S(\mathbf{k}_2, \omega_2)}{1 + \alpha(\omega) U(\mathbf{k})} \times E(\mathbf{k}_1, \omega_1) E(\mathbf{k}_2, \omega_2) = \rho_0 \beta(\omega_1, \omega_2) S(\mathbf{k}_1, \omega_1) S(\mathbf{k}_2, \omega_2) S(\mathbf{k}, \omega) \times E(\mathbf{k}_1, \omega_1) E(\mathbf{k}_2, \omega_2)$$

$$= \chi^{(2)}(-\mathbf{k}, -\omega; \mathbf{k}_1, \omega_1, \mathbf{k}_2, \omega_2) \times E(\mathbf{k}_1, \omega_1) E(\mathbf{k}_2, \omega_2). \quad (14)$$

Here in Eq. (14), the third equality is just a definition of the second-order susceptibility. Therefore, we find that the second-order nonlinear susceptibility is related to the molecular first hyperpolarizability as

$$\chi^{(2)}(-\mathbf{k}, -\omega; \mathbf{k}_1, \omega_1, \mathbf{k}_2, \omega_2) = \rho_0 \beta(\omega_1, \omega_2) S(\mathbf{k}_1, \omega_1) S(\mathbf{k}_2, \omega_2) S(\mathbf{k}, \omega). \quad (15)$$

This will be used to theoretically study the coverage dependence of the IV-SFG signal from CO molecules adsorbed on the Ru metal surface.

C. Third-order nonlinear susceptibility

Now, it is a straightforward exercise to carry out the calculation of the third-order susceptibility following the same procedure above. After some algebra, we find that the third-order susceptibility is given by a sum of direct and cascading contributions,

$$\chi^{(3)}(-\mathbf{k}, -\omega; \mathbf{k}_1, \omega_1, \mathbf{k}_2, \omega_2, \mathbf{k}_3, \omega_3) = \chi_{\text{dir}}^{(3)} + \chi_{\text{cas}}^{(3)}, \quad (16)$$

where

$$\chi_{\text{dir}}^{(3)}(-\mathbf{k}, -\omega; \mathbf{k}_1, \omega_1, \mathbf{k}_2, \omega_2, \mathbf{k}_3, \omega_3) = \rho_0 \gamma(\omega_1, \omega_2, \omega_3) S(\mathbf{k}_1, \omega_1) S(\mathbf{k}_2, \omega_2) S(\mathbf{k}_3, \omega_3) S(\mathbf{k}, \omega) \quad (17)$$

and

$$\chi_{\text{cas}}^{(3)}(-\mathbf{k}, -\omega; \mathbf{k}_1, \omega_1, \mathbf{k}_2, \omega_2, \mathbf{k}_3, \omega_3) = \rho_0 [\beta(\omega_1, \omega_2) \beta(\omega_1 + \omega_2, \omega_3) T(\mathbf{k}_1 + \mathbf{k}_2, \omega_1 + \omega_2) + \beta(\omega_1, \omega_3) \beta(\omega_1 + \omega_3, \omega_2) T(\mathbf{k}_1 + \mathbf{k}_3, \omega_1 + \omega_3) + \beta(\omega_2, \omega_3) \beta(\omega_2 + \omega_3, \omega_1) T(\mathbf{k}_2 + \mathbf{k}_3, \omega_2 + \omega_3)] \times S(\mathbf{k}_1, \omega_1) S(\mathbf{k}_2, \omega_2) S(\mathbf{k}_3, \omega_3) S(\mathbf{k}, \omega). \quad (18)$$

Here the auxiliary function $T(\mathbf{k}, \omega)$ is defined as

$$T(\mathbf{k}, \omega) \equiv -U(\mathbf{k}) S(\mathbf{k}, \omega). \quad (19)$$

The direct third-order nonlinear optical process is determined by the molecular second hyperpolarizability $\gamma(\omega_1, \omega_2, \omega_3)$, whereas the cascading contributions are related to the first-hyperpolarizability terms.

III. EXPERIMENT

The surface vibrational spectroscopies used in this study are infrared-visible sum-frequency generation (IV-SFG) and its extension to infrared-infrared-visible sum-frequency generation (IIV-SFG), applied to the C-O-stretch vibration of CO adsorbed on Ru(001) as a function of coverage. The

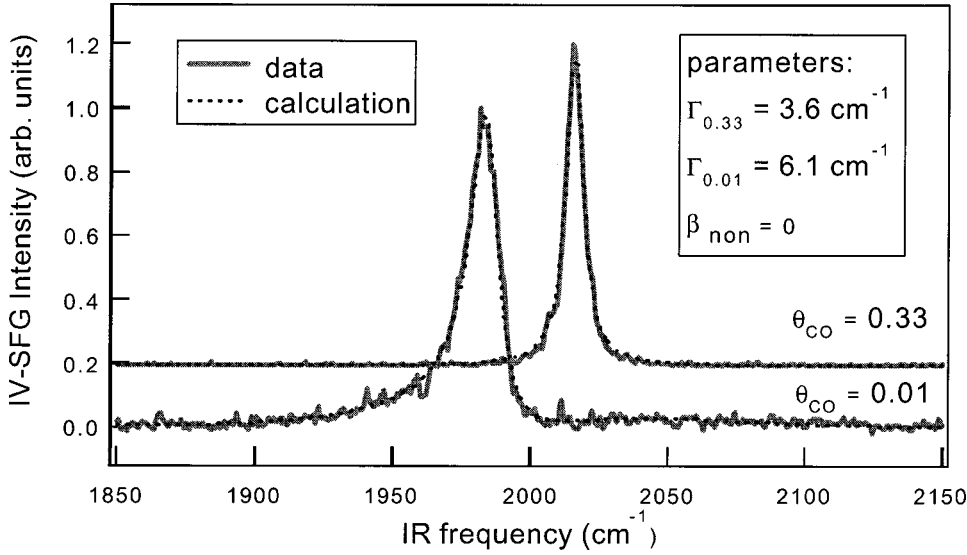


FIG. 1. Normalized experimental IV-SFG spectra of CO on Ru(001) for two different coverages indicated in the graph. The theoretical fits to the experimental data were made using Eq. (24) for the nonlinear susceptibility, with parameters $\alpha_e = 3.2 \text{ \AA}^3$, $\alpha_v = 0.52 \text{ \AA}^3$, $\omega_0 = 1982.1 \text{ cm}^{-1}$, and $U_0 = 0.082 \text{ \AA}^{-3}$. The line-width was observed to vary from $\Gamma = 6.1$ to 3.6 cm^{-1} , with increasing coverage (as has been observed previously in infrared-absorption measurements). The high-coverage measurement is offset for clarity.

Ru(001) sample is mounted in an ultrahigh vacuum chamber (UHV, base pressure $< 1 \times 10^{-10}$ mbar; equipped with standard surface science tools). A detailed description of the UHV and optical setup together with the surface cleaning, preparation, and characterization procedures are given in Ref. 44. The experiments were performed at a sample temperature of 100 K.

For the experiments a femtosecond laser system was used, delivering 800-nm, 110-fs pulses with a pulse energy of 4 mJ per pulse at 400 Hz. Part of the output is used to pump an optical parametric generator/optical parametric amplifier (OPG/OPA) with subsequent difference frequency mixing of the signal and idler of the OPA to generate tunable IR radiation (2–10 μm) with a bandwidth of about 100 cm^{-1} (full width at half maximum) and a pulse energy of up to 25 μJ . The frequency of the IR pulses is chosen to be resonant with the $^{12}\text{C}^{16}\text{O}$ -stretch frequency of CO adsorbed on Ru(001). The residual 800-nm radiation, which is not converted in the parametric process, was spectrally shaped to provide narrow-bandwidth visible (VIS) pulses, with a pulse energy of 4 μJ , that are used to up-convert the IR pulses in the SFG experiments. The IR and visible pulses are brought to temporal and spatial overlap on the surface with the IR pulses having an incident angle of 75° with respect to the surface normal. The focus of the IR beam, 300- μm in diameter, is within the spot size of the visible beam. The SFG beam reflected from the surface is focused into a spectrograph with a 1200-gr/mm grating and dispersed across an intensified charge coupled device detector. The infrared pulse energy was kept suffi-

ciently low to avoid effects of saturation in the IV-SFG experiments. In the IIV-SFG experiments higher energies were used due to the low signal level, in some cases leading to an inconsequential broadening of the IIV resonance.

IV. FRACTIONAL COVERAGE DEPENDENCE OF THE IR-VIS SUM-FREQUENCY GENERATION IV-SFG

Figure 1 depicts the IV-SFG data for coverages of 0.01 and 0.33 ML. There is a pronounced blueshift in the resonance with increasing coverage as a result of the intermolecular interaction. This blueshift, in addition to the changes in integrated intensity of the IV-SFG signal, will be the focus of our theoretical efforts. In contrast, the variation in the width of the resonance will not be discussed, since it is outside the scope of our theory.

The IR absorption of CO on metal surfaces has been investigated extensively over the last two decades and the fractional coverage dependence of the IR-absorption spectrum was reproduced theoretically using the expression in Eq. (9) in the long-wavelength ($\mathbf{k}=0$) limit.^{42,43,45–49} However, to our best knowledge, a theoretical analysis of the fractional coverage dependence of the IV-SFG spectrum does not exist. In this section, we will use the expression for the second-order nonlinear susceptibility in Eq. (15) to quantitatively describe the screening effect on the IV-SFG process of CO molecules on metal surfaces, and apply the theory to the CO/Ru(001) system.

From Eq. (15), the IV-SFG susceptibility can be written as

$$\chi_{\text{IV-SFG}}^{(2)} = \frac{\rho_0 \beta(\omega_1, \omega_2)}{[1 + \alpha(\omega_1)U(\mathbf{k}_1)][1 + \alpha(\omega_2)U(\mathbf{k}_2)][1 + \alpha(\omega_{\text{IV-SFG}})U(\mathbf{k})]}, \quad (20)$$

where $\mathbf{k} = \mathbf{k}_{\text{ir}} + \mathbf{k}_{\text{vis}}$ and $\omega_{\text{IV-SFG}} = \omega_{\text{ir}} + \omega_{\text{vis}}$. The molecular polarizability can be written as a sum of the electronic and vibrational contributions, i.e.,

$$\alpha(\omega) = \alpha_e + \frac{\alpha_v}{1 - (\omega/\omega_0)^2 + 2i\Gamma}, \quad (21)$$

where the vibrational frequency of the CO-stretching mode for an isolated (from other CO molecules) CO molecule on a metal surface is denoted as ω_0 , and the vibrational dephasing constant is denoted as Γ . The full width at half maximum of the Lorentzian line-shape function is 2Γ in this case. The electronic and vibrational polarizabilities are denoted as α_e and α_v in Eq. (21).

Since the IR and visible field frequencies are much larger than the vibrational frequency and the visible field is far off resonant with the electronic transition of CO molecules, we can make the following approximations:

$$\alpha(\omega_{\text{vis}}) \cong \alpha_e$$

and

$$\alpha(\omega_{\text{IV-SFG}}) \cong \alpha_e. \quad (22)$$

Since the magnitudes of the IR and visible wave vectors are negligibly small in comparison to the length scale of the system, $|\mathbf{k}_{\text{ir}}| = |\mathbf{k}_{\text{vis}}| \cong 0$, the IV-SFG susceptibility in Eq. (20) can be simplified to

$$\chi_{\text{IV-SFG}}^{(2)}(\omega_{\text{ir}}) \cong \frac{\rho_0 \beta(\omega_{\text{ir}}, \omega_{\text{vis}})}{[1 + \alpha(\omega_{\text{ir}})U_0][1 + \alpha_e U_0]^2}, \quad (23)$$

where $U_0 \equiv U(\mathbf{k}=0)$.

Now, in analogy to the theoretical procedure developed by Persson and Ryberg in Ref. 45, for an *incomplete* monolayer the IV-SFG susceptibility, Eq. (23), can be approximated by

$$\chi_{\text{IV-SFG}}^{(2)}(\theta, \omega_{\text{ir}}) \cong \frac{c \beta(\omega_{\text{ir}}, \omega_{\text{vis}})}{[1 + c \alpha(\omega_{\text{ir}})U_0][1 + c \alpha_e U_0]^2}. \quad (24)$$

Here, we postulate that the complete monolayer corresponds to a fractional coverage of 0.33 ML, since we are only interested in coverages below 0.33 ML. Thus, the coverage of the adsorbed molecules, denoted as c , varies from 0 to 1, as the fractional coverage increases from 0 to 0.33 ML.

Here we should emphasize that we only consider incomplete monolayers with fractional coverage varying from 0 to 0.33 ML. At $\theta=0.33$, the adsorbed CO molecules form a well-ordered ($\sqrt{3} \times \sqrt{3}$) structure. Within this range of fractional coverages, the dipole sum factor $U_0 = U(\mathbf{k}=0)$ can be assumed to be a constant. However, it is well known that there exists another ordered, $2\sqrt{3}$ structure at $\theta=0.68$ ML.⁴² However, in this case, the assumption that U_0 is constant is no longer valid. Thus, in the present paper, we will restrict our experimental and theoretical investigation to coverages ranging from 0 to 0.33 ML.

In order to reproduce the experimental data using Eq. (24), we first have to obtain an expression for the first hyperpolarizability $\beta(\omega_{\text{ir}}, \omega_{\text{vis}})$. Since the visible field is electronically off resonant and the IR field is vibrationally resonant, $\beta(\omega_{\text{ir}}, \omega_{\text{vis}})$ can be approximated by²

$$\beta(\omega_{\text{ir}}, \omega_{\text{vis}}) = \beta_{\text{non}} + \frac{\beta_{\text{res}}}{1 - \omega_{\text{ir}}/\omega_0 - i\Gamma/\omega_0}. \quad (25)$$

In Eq. (25), the vibrationally resonant and nonresonant terms were denoted as β_{res} and β_{non} , respectively. Here, it is

assumed that the electronic (nonresonant) first hyperpolarizability is independent of IR frequency, and that this approximation is quantitatively reliable.

Although, as will be shown below, the resonant part of the hyperpolarizability is much larger than the nonresonant part, $\beta_{\text{res}} \gg \beta_{\text{non}}$, there is also a background nonresonant contribution to the signal from the underlying metal, arising from the metal contribution to the nonlinear susceptibility $\chi_{\text{metal}}^{(2)}$, which can be approximated by $\chi_{\text{metal}}^{(2)} = B e^{i\phi}$, with ϕ being the relative phase between the molecular response and that of the metal. The linewidth Γ is a free parameter in the calculation.

The results of this calculation using Eqs. (24) and (25) are depicted as dashed lines in Fig. 1 along with the experimental spectra. Because of the nonzero phase factor $e^{i\phi}$, associated with the electronic contribution to the total IV-SFG susceptibility from the metal substrate, the spectrum at $\theta = 0.01$ is slightly asymmetric. However, as the relative importance of the vibrationally resonant term increases with increasing coverage, the IV-SFG spectrum becomes symmetric for higher coverages (from which it can be concluded that $\beta_{\text{non}} \ll \beta_{\text{res}}$, since at higher coverages there is no indication for a molecular nonresonant response in the IV-SFG spectrum). The best fit (depicted as a dashed line in Fig. 1) was obtained when the vibrational dephasing constant of CO on the Ru(001) surface Γ equals 6.1 and 3.6 cm^{-1} for $\theta=0.01$ and 0.33 ML. These values are somewhat larger than that obtained from the IR-absorption spectrum due to the finite experimental spectral resolution. The procedure for obtaining the parameters α_e , α_v , ω_0 , and U_0 , necessary to reproduce the high-coverage spectrum, will be described below. Note that for the low-coverage spectrum only the hyperpolarizability and the metal response determine the signal.

We shall use $\Gamma = 6.1 \text{ cm}^{-1}$ for the theoretical analysis of the IV- and IIV-SFG spectra throughout this paper, unless otherwise indicated. Where necessary, we have corrected (e.g., the integrated intensity) for the coverage-dependent linewidth.

Next, we will determine various parameters required for fitting the experimental data with the theoretical expression for the IV-SFG signal. From the definition of the linear polarizability given in Eq. (21), the resonant and nonresonant polarizabilities, as well as ω_0 , should be determined. Recently, the first two quantities, α_e and α_v , were determined by using the IR-absorption measurement of the same composite system, and they have been found to be⁵⁰

$$\alpha_e = 3.2 \text{ \AA}^3$$

and

$$\alpha_v = 0.52 \text{ \AA}^3. \quad (26)$$

The fundamental transition frequency ω_0 of a single CO molecule on the Ru surface can be determined by using the IV-SFG measurement in the low fractional coverage limit. The experimentally measured center frequencies of the IV-SFG spectra for $0 < \theta < 0.5$ are depicted in Fig. 2. From the experimental data, we find

$$\omega_0 = 1982.1 \text{ cm}^{-1}. \quad (27)$$

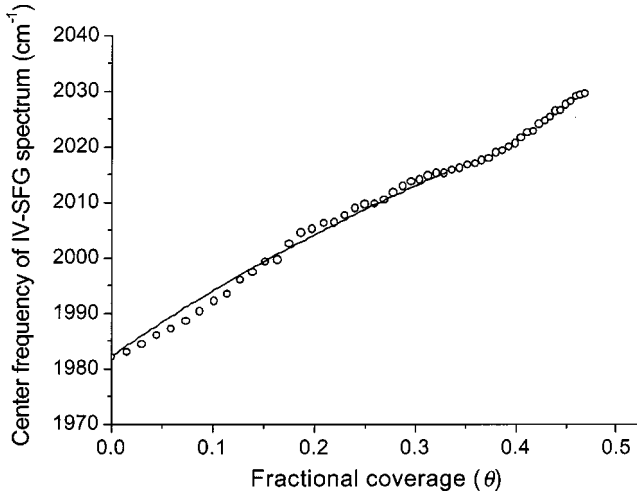


FIG. 2. The experimentally measured center frequency of the IV-SFG spectrum (open circles). The solid curve corresponds to the theoretical fitting result with the same parameters that were used to describe the data in Fig. 1: $\alpha_e = 3.2 \text{ \AA}^3$, $\alpha_v = 0.52 \text{ \AA}^3$, $\omega_0 = 1982.1$, $\Gamma = 6.1 \text{ cm}^{-1}$, and $U_0 = 0.082 \text{ \AA}^{-3}$.

Finally, the dipole sum U_0 should be determined. By using the IV-SFG susceptibility given in Eq. (24) with parameters α_e , α_v , Γ , and ω_0 , determined above, the center frequency of the measured IV-SFG spectrum can be calculated. For the best fit, we find

$$U_0 = 0.082 \text{ \AA}^{-3}. \quad (28)$$

In Fig. 2, the theoretically calculated center frequency as a function of the fractional coverage is plotted and compared with experiment. Although this value, $U_0 = 0.082 \text{ \AA}^{-3}$, is slightly smaller than that estimated from IR-absorption measurements,⁴⁵ the set of parameters determined above provides excellent results for the integrated intensities of the IV- and IIV-SFG signals as well as the center frequency of the IIV-SFG spectra as functions of the fractional coverage, as will be shown later in this paper.

By using these parameters and assuming that the dephasing constant Γ does not depend on the fractional coverage, the IV-SFG spectra with respect to the fractional coverage are plotted in Fig. 3. This figure demonstrates the blueshift and increase in integrated intensity that occurs with increasing coverage. The experimentally measured integrated intensities of the IV-SFG spectra with respect to the fractional coverage are plotted in Fig. 4. The experimental data have been corrected for the coverage-dependent linewidth (see Fig. 1), which presents a trivial effect on the intensity that is not incorporated in the theory. Although the experimental data are slightly scattered, the agreement between theory and experiment is satisfactory. It should be noted that the calculated integrated intensity is completely determined by using the set of parameters already determined above. Note also the sudden drop in integrated intensity for $\theta > 0.33 \text{ ML}$, which is caused by the fact that U_0 is no longer constant, as mentioned above. This behavior is outside the scope of the theory presented here.

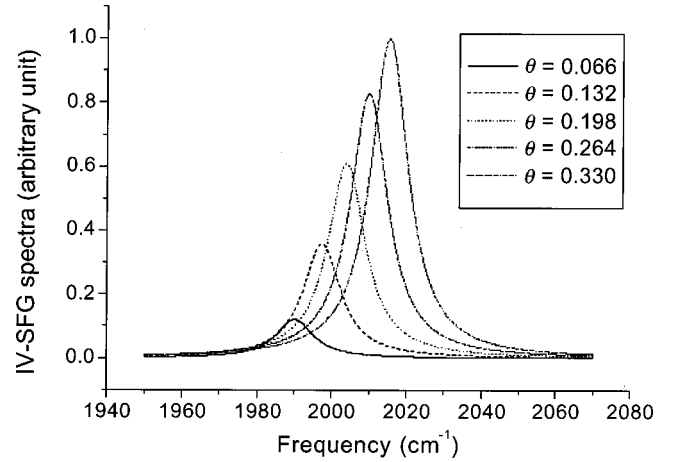


FIG. 3. The calculated IV-SFG spectra as a function of fractional coverage. From left to right, $\theta = 0.066$, 0.132 , 0.198 , 0.264 , and 0.33 , respectively. The parameters that were used in the calculation are given in the caption of Fig. 2.

V. FRACTIONAL COVERAGE DEPENDENCE OF THE IR-IR-VIS SUM-FREQUENCY (IIV-SFG) SIGNAL

Figure 5 depicts three IIV-SFG spectra: two spectra at coverages of 0.33 and 0.2 and one for which the signal was integrated for coverages from 0 to 0.1 ML . Remarkably, the resonant signal does not appear until a coverage of $\sim 0.12 \text{ ML}$, indicating a very strong nonlinearity in the resonant response vs coverage. In analogy to the IV-SFG measurements, a pronounced blueshift of the resonance is observed with increasing coverage. As pointed out previously,³⁹ the resonant peak in the IIV-SFG signal is located at twice the frequency of the fundamental.

IIV-SFG spectroscopy, which was theoretically proposed as two-dimensional vibrational spectroscopy in an isotropic system,²⁷ was used by Bonn *et al.*³⁹ to investigate the vibra-

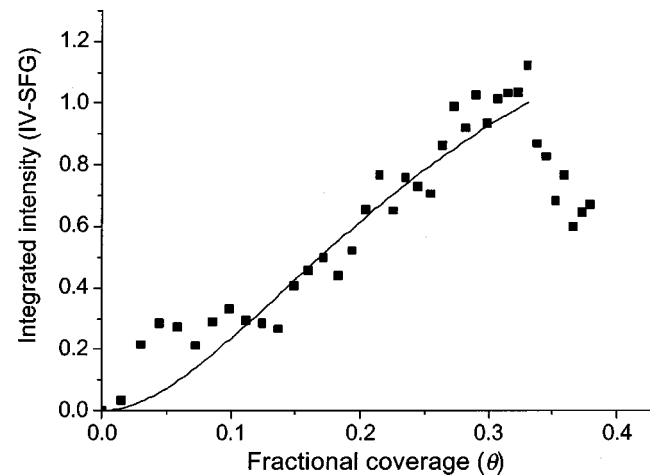


FIG. 4. The experimentally determined integrated intensities of the IV-SFG spectra with respect to the fractional coverage from 0 to 0.4 (filled squares). The intensity is rescaled to make the fit with the theoretically predicted integrated intensity, which is represented by the solid curve. Other than this rescaling factor, there are no adjustable parameters in this calculation.

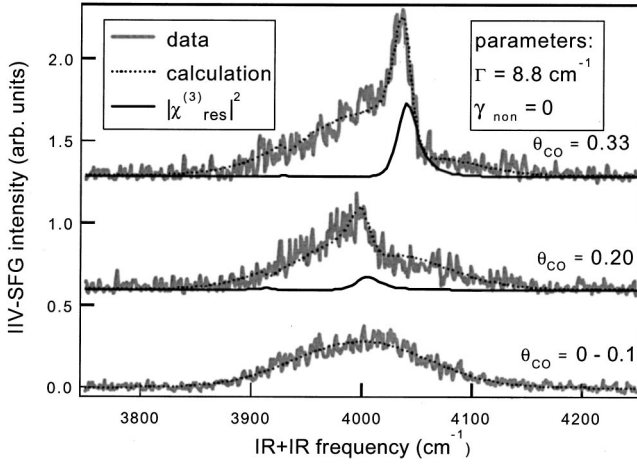


FIG. 5. Experimental IIV-SFG spectra for different fractional coverages (gray lines). Note that below a coverage of 0.1 ML, no resonant signal can be observed, indicating a strong nonlinearity of the resonant signal vs coverage. The dashed lines show fits to Eq. (33) [with γ from Eq. (35)] and with parameters indicated in the caption of Fig. 2 and the graph, to the resonant part of the susceptibility.

tional interactions between adsorbed CO molecules on a transition-metal surface. Although the report in Ref. 39 demonstrates that this method can be a useful tool for the investigation of the vibrational coupling between adsorbed molecules, the theoretical analysis presented in Ref. 39 was incomplete because it was based on the localized mode picture. In the present section, a new theoretical framework for the interpretation of the IIV-SFG spectroscopy of adsorbed molecules on surfaces will be provided using the general theory discussed in Sec. II.

For the IIV-SFG experiment, the two-IR field frequencies are assumed to be independently controllable and the following notations will be used,

$$\omega_1 = \omega_{\text{ir},1}, \quad \omega_2 = \omega_{\text{ir},2}, \quad \omega_3 = \omega_{\text{vis}}. \quad (29)$$

The wave vector and frequency of the IIV-SFG field are, respectively,

$$\mathbf{k} = \mathbf{k}_1 + \mathbf{k}_2 + \mathbf{k}_3, \quad \omega_{\text{IIV-SFG}} = \omega_1 + \omega_2 + \omega_3. \quad (30)$$

Since the visible field frequency is far from resonance with electronic as well as vibrational transitions, the following approximations can be made:

$$\begin{aligned} \alpha(\omega_3) &\cong \alpha_e, & \alpha(\omega_1 + \omega_3) &= \alpha(\omega_2 + \omega_3) \cong \alpha_e, \\ \alpha(\omega_{\text{IIV-SFG}}) &\cong \alpha_e. \end{aligned} \quad (31)$$

Then, from Eq. (16), the IIV-SFG susceptibility can be written in terms of the molecular first and second hyperpolarizabilities as

$$\chi_{\text{IIV-SFG}}^{(3)} = \chi_{\text{IIV-SFG}}^{\text{dir}} + \chi_{\text{IIV-SFG}}^{\text{cas}}, \quad (32)$$

where

$$\begin{aligned} \chi_{\text{IIV-SFG}}^{\text{dir}} &\propto \frac{c \gamma(\omega_1, \omega_2, \omega_3)}{[1 + c \alpha(\omega_1) U_0][1 + c \alpha(\omega_2) U_0][1 + c \alpha_e U_0]^2}, \quad (33) \\ \chi_{\text{IIV-SFG}}^{\text{cas}} &\propto \left[c^2 \beta(\omega_1, \omega_2) \beta(\omega_1 + \omega_2, \omega_3) \right. \\ &\quad \times \left\{ \frac{U_0}{1 + c \alpha(\omega_1 + \omega_2) U_0} \right\} \\ &\quad + c^2 \beta(\omega_1, \omega_3) \beta(\omega_1 + \omega_3, \omega_2) \left\{ \frac{U_0}{1 + c \alpha_e U_0} \right\} \\ &\quad \left. + c^2 \beta(\omega_2, \omega_3) \beta(\omega_2 + \omega_3, \omega_1) \left\{ \frac{U_0}{1 + c \alpha_e U_0} \right\} \right] \\ &\quad \times \frac{1}{[1 + c \alpha(\omega_1) U_0][1 + c \alpha(\omega_2) U_0][1 + c \alpha_e U_0]^2}. \quad (34) \end{aligned}$$

Since in principle the two-infrared field frequencies are independently tunable, the measured susceptibility or IIV-SFG signal intensity can be displayed in the two-dimensional (2D) frequency space. Thus, not only the diagonal peaks but also the off-diagonal peaks can be measured by scanning the two-IR frequencies.

Due to the screening factors in Eqs. (33) and (34), not only the precise location of the 2D peak but also the integrated intensity will be notably different for different fractional coverage. In order to carry out a numerical simulation of the IIV-SFG signal, we need to differentiate the two contributions, i.e., the direct IIV-SFG term and the cascading terms, separately.

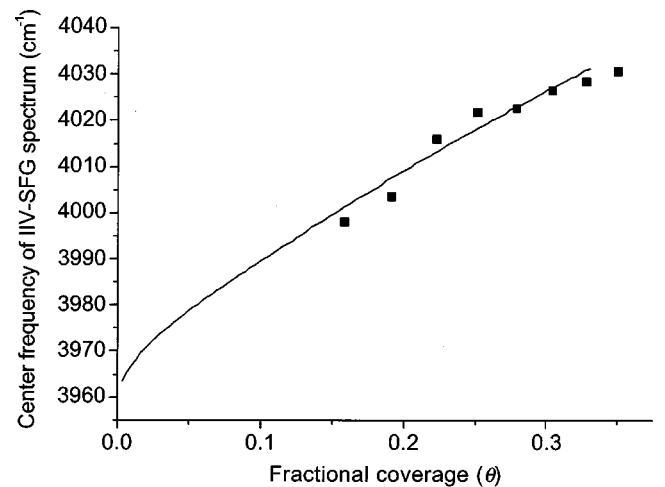


FIG. 6. Experimentally measured center frequencies of the IIV-SFG spectra for different fractional coverages (filled squares). As mentioned in the text, the absolute value of the center frequency of the IIV-SFG spectrum cannot be determined from the experiment, whereas the frequency shift can. Therefore, in order to make a comparison with the theory, we added a constant to the measured frequency shift for the purpose of fitting. The solid curve is the theoretically calculated center frequency.

Since the total signal is proportional to the absolute square of the susceptibility, the interference between the two distinctive contributions $\chi_{\text{IIV-SFG}}^{\text{dir}}$ and $\chi_{\text{IIV-SFG}}^{\text{cas}}$ may also play a role. However, as discussed in detail in Ref. 39, the cascading contribution can be safely ruled out in comparison to the direct IIV-SFG contribution for the CO Ru(001) system.

Although the expression for $\chi_{\text{IIV-SFG}}^{\text{dir}}$ in Eq. (33) is the case of the general two-color IIV-SFG susceptibility, we will spe-

cifically consider one-color (degenerate) IIV-SFG because the recent IIV-SFG experiment was performed using one IR beam to create a two-IR quantum coherence state. With help of the theory from Ref. 27, the *molecular* second hyperpolarizability $\gamma(\omega_1, \omega_2, \omega_3)$, which represents the IR-IR-VIS sum-frequency generation by an isolated (from the other adsorbed molecules) CO molecule adsorbed on a surface, can be written as

$$\gamma(\omega_{\text{ir}}, \omega_{\text{ir}}, \omega_{\text{vis}}) = \gamma_{\text{non}} + \frac{\gamma_{\text{res}}}{(1 - \omega_{\text{ir}}/\omega_0 - i\Gamma/\omega_0)(2 - \Delta/\omega_0 - 2\omega_{\text{ir}}/\omega_0 - 2i\Gamma/\omega_0)}, \quad (35)$$

where the vibrationally nonresonant and resonant parts are weighted by γ_{non} and γ_{res} , respectively. If the molecular eigenstates of a CO stretch are denoted as $|0\rangle$, $|1\rangle$, and $|2\rangle$, the IIV-SFG process of a single molecule involves a sequence of vibrational transitions, i.e., $|0\rangle \rightarrow |1\rangle \rightarrow |2\rangle \rightarrow |0\rangle$. Although the first transition frequency is ω_0 , the second transition frequency from $|1\rangle$ to $|2\rangle$ is $\omega_0 - \Delta$, where Δ is related to the molecular anharmonicity. This quantity, Δ , was already estimated to be 54.4 cm^{-1} so that $\omega_0 = 1982.1$ and $2\omega_0 - \Delta = 3909.8 \text{ cm}^{-1}$.^{51,52}

The data in Fig. 5 are fitted with Eq. (33) and (35) in conjunction with a nonresonant background from the metal surface, which can be recorded independently at low CO coverages (lower trace in Fig. 5). In analogy to the IV-SFG spectra where the nonresonant hyperpolarizability was negligibly small, we find that $\gamma_{\text{non}} \ll \gamma_{\text{res}}$ for the IIV-SFG spectra. The solid lines in Fig. 5 represent the molecular contribution to the third-order susceptibility. The center frequency vs coverage is plotted in Fig. 6, and the integrated *resonant* intensity in Fig. 7. The theoretically calculated center frequencies of the IIV-SFG spectrum as a function of the fractional coverage are also plotted in Fig. 6. For the experimental IIV-SFG spectra, although the absolute location of the center frequency can be determined with an accuracy of only $\sim 10 \text{ cm}^{-1}$, the sensitivity to the relative shift of the peak frequency is much higher. For the experimental data shown in Fig. 6 as filled squares, an offset value was added to the measured relative shift data to compare data and theory. The agreement is very good.

Considering the integrated intensity of the IIV-SFG signal, it can be observed in Fig. 5 that, surprisingly, no resonant response is observed until the coverage exceeds 0.12 ML. The strong nonlinearity of the integrated intensity as a function of the fractional coverage is summarized in Fig. 7. The solid line indicates the calculation of the intensity using the same set of parameters mentioned above. Also here, the agreement is found to be quantitative. Note that we have now reproduced, for both the IV- and IIV-SFG, the experimental spectra, the coverage dependence of the center frequency, and the integrated intensity (i.e., six data sets) with one set of parameters.

Before closing this section, we would like to point out the advantage of nonlinear vibrational spectroscopic methods for the investigation of the vibrational interaction between adsorbed molecules on a metal surface. Although most of the parameters required in the fitting can be determined using linear IR-absorption spectroscopy, the nonlinear molecular properties such as the first and second hyperpolarizabilities of CO on Ru(001) can only be studied by using the nonlinear vibrational spectroscopies discussed in this paper, due to the inherent nonlinear character of IV- and IIV-SFG. The advantage of using the IIV-SFG method over the conventional IV-SFG method lies in its power to be used as a two-dimensional spectroscopic tool. As mentioned in the Introduction, the IIV-SFG is inherently a two-dimensional vibrational spectroscopy, though in this paper only one-color IR pulse was employed in the IIV-SFG experiment. If two IR fields are tuned to be resonant with two different vibrational chromophores on a metal surface, the IIV-SFG spectrum can be displayed in the two-dimensional frequency space. The resultant spectrum will exhibit not only the diagonal peaks but also off-diagonal (cross) peaks. Particularly, the intensity

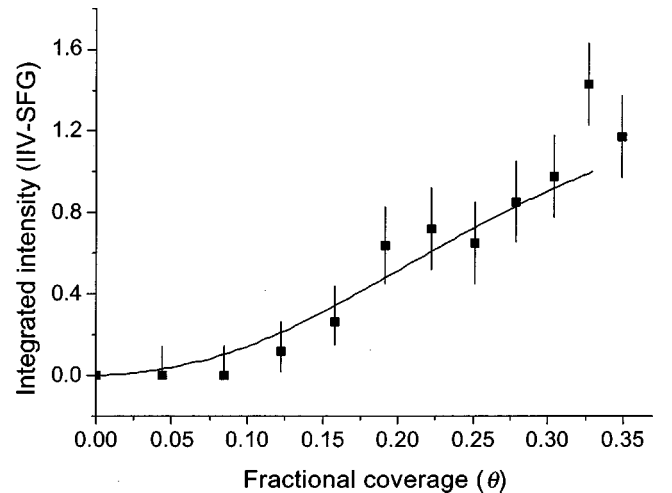


FIG. 7. The experimentally determined integrated intensity of the IIV-SFG spectra vs surface coverage (plotted as filled squares), and the theoretical calculation results with the parameters given in the caption of Fig. 2 (solid curve).

and location of the cross peak will be of importance since they carry information on the vibrational coupling strength between two different chromophores. To the best of the authors' knowledge, there do not exist theoretical formulations of the IV- and IIV-SFG susceptibilities of adsorbed molecules on a metal surface taking into account the screening effects, which are induced by the lateral interactions between adsorbates on surfaces, on the nonlinear optical susceptibilities. Thus, the theoretical formulations presented in this paper will be a valuable starting point for further investigation of vibrational interactions between distinctly different chemical species on a metal surface via nonlinear vibrational spectroscopic methods considered in this paper.

VI. SUMMARY

In conclusion, we have presented experimental and theoretical investigations into the vibrational coupling of molecules adsorbed on surfaces using second- and third-order nonlinear vibrational techniques. Experimentally, the strength of the intermolecular interaction can be tuned by changing the surface coverage. The interaction has pro-

nounced effects on the vibrational signals, in particular resulting in a shift of the center frequency and a nonlinear increase in integrated intensity with increasing coverage. To describe these results, analytic expressions are derived for the nonlinear susceptibilities in terms of molecular (hyper)polarizabilities. Excellent agreement is obtained between this theory and the experimental results. These results indicate that the dominant effect on the nonlinear susceptibilities is the local-field correction for the linear infrared field.

ACKNOWLEDGMENTS

M.C. is grateful for the support from KISTEP via the Creative Research Initiatives Program (MOST, Korea). M.B. acknowledges support from the Royal Netherlands Academy of Arts and Sciences KNAW and from the Netherlands Science Organization NWO. We are very grateful to Martin Wolf for experimental and other support. Also, we gratefully acknowledge Professor G. Ertl for continuous support and James H. Miners for experimental help.

*Corresponding author. Email address: mcho@korea.ac.kr

- ¹Y. R. Shen, in *Frontier in Laser Spectroscopy*, Proceedings of the International School of Physics "Enrico Fermi," Course CXX, edited by T. W. Hensch and M. Inguscio (North-Holland, Amsterdam, 1994), p. 139.
- ²X. D. Zhu, H. Suhr, and Y. R. Shen, *Phys. Rev. B* **35**, 3047 (1987).
- ³P. Guyot-Sionnest, J. H. Hunt, and Y. R. Shen, *Phys. Rev. Lett.* **59**, 1597 (1987).
- ⁴R. Superfine, J. Y. Huang, and Y. R. Shen, *Phys. Rev. Lett.* **66**, 1066 (1991).
- ⁵Y. R. Shen, *Surf. Sci.* **299/300**, 551 (1994).
- ⁶S. H. Lin and A. A. Villaeys, *Phys. Rev. A* **50**, 5134 (1994).
- ⁷Y. R. Shen, *Nature (London)* **337**, 519 (1989), and references therein.
- ⁸T. Kato, M. Hayashi, A. A. Villaeys, and S. H. Lin, *Phys. Rev. A* **56**, 980 (1997).
- ⁹T. F. Heinz, F. J. Himpsel, E. Palange, and E. Burstein, *Phys. Rev. Lett.* **63**, 644 (1989).
- ¹⁰M. Y. Jiang, G. Pajer, and E. Burstein, *Surf. Sci.* **242**, 306 (1991).
- ¹¹Y. J. Chabal, *Surf. Sci. Rep.* **8**, 211 (1988).
- ¹²E. J. Heilweil, M. P. Casassa, R. R. Cavanagh, and J. C. Stephenson, *Annu. Rev. Phys. Chem.* **40**, 143 (1989).
- ¹³A. L. Harris and N. J. Levinos, *J. Chem. Phys.* **90**, 3878 (1989).
- ¹⁴A. L. Harris, L. Rothberg, L. H. Dubois, N. J. Levinos, and L. Dhar, *Phys. Rev. Lett.* **64**, 2086 (1990); A. L. Harris and L. Rothberg, *J. Chem. Phys.* **94**, 2449 (1991).
- ¹⁵M. Morin, N. J. Levinos, and A. L. Harris, *J. Chem. Phys.* **96**, 3950 (1992).
- ¹⁶K. Kuhnke, M. Morin, P. Jakob, N. L. Levinos, Y. J. Chabal, and A. L. Harris, *J. Chem. Phys.* **99**, 6114 (1993).
- ¹⁷A. Peremans and A. Tadjeddine, *Phys. Rev. Lett.* **73**, 3010 (1994).
- ¹⁸J. D. Beckerle, R. R. Cavanagh, M. P. Casassa, E. J. Heilweil, and J. C. Stephenson, *J. Chem. Phys.* **95**, 5403 (1991).
- ¹⁹P. Guyot-Sionnest, P. Dumas, Y. J. Chabal, and G. H. Higashi, *Phys. Rev. Lett.* **64**, 2156 (1990).
- ²⁰P. Guyot-Sionnest, *Phys. Rev. Lett.* **66**, 1489 (1991).
- ²¹R. P. Chin, J. Y. Huang, Y. R. Shen, T. J. Chuang, H. Seki, and M. Buck, *Phys. Rev. B* **45**, 1522 (1992).
- ²²D. E. Gragson and G. L. Richmond, *J. Chem. Phys.* **107**, 9687 (1997).
- ²³S. Baldelli, C. Schnitzer, and M. J. Shultz, *J. Chem. Phys.* **108**, 9817 (1998).
- ²⁴M. E. Schmidt and P. Guyot-Sionnest, *J. Chem. Phys.* **104**, 2438 (1996).
- ²⁵M. Bonn, Ch. Hess, S. Funk, J. H. Miners, B. N. J. Persson, M. Wolf, and G. Ertl, *Phys. Rev. Lett.* **84**, 4653 (2000).
- ²⁶K. Park and M. Cho, *J. Chem. Phys.* **109**, 10 559 (1998).
- ²⁷M. Cho, *Phys. Rev. A* **61**, 023406 (2000).
- ²⁸Y. Tanimura and S. Mukamel, *J. Chem. Phys.* **99**, 9496 (1993).
- ²⁹M. Cho, in *Advances in Multi-Photon Processes and Spectroscopy*, edited by S. H. Lin, A. A. Villaeys, and Y. Fujimura (World Scientific, Singapore, 1999), Vol. 12, p. 229.
- ³⁰S. Mukamel, A. Piryatinski, and V. Chernyak, *Acc. Chem. Res.* **32**, 145 (1999).
- ³¹K. Tominaga, G. P. Keogh, Y. Naitoh, and K. Yoshihara, *J. Raman Spectrosc.* **26**, 495 (1995); K. Tominaga and K. Yoshihara, *Phys. Rev. Lett.* **74**, 3061 (1995); *ibid.* **76**, 987 (1996); *J. Chem. Phys.* **104**, 1159 (1996); *ibid.* **104**, 4419 (1996).
- ³²T. Steffen and K. Duppen, *J. Chem. Phys.* **106**, 3854 (1997); *Phys. Rev. Lett.* **76**, 1224 (1996); T. Steffen, J. T. Fourkas, and K. Duppen, *J. Chem. Phys.* **105**, 7364 (1996).
- ³³D. Blank, L. Kaufman, and G. R. Fleming, *J. Chem. Phys.* **113**, 771 (2000); L. Kaufman, D. Blank, and G. R. Fleming, *ibid.* **114**, 2312 (2001).
- ³⁴J. Sung and M. Cho, *J. Chem. Phys.* **113**, 7072 (2000); J. Sung, R. J. Silbey, and M. Cho, *ibid.* **115**, 1422 (2001).
- ³⁵W. Zhao and J. C. Wright, *Phys. Rev. Lett.* **83**, 1950 (1999); *J. Am. Chem. Soc.* **121**, 10 994 (1999); *Phys. Rev. Lett.* **84**, 1411 (2000).

- ³⁶P. Hamm, M. Lim, and R. Hochstrasser, *J. Chem. Phys.* **112**, 1907 (2000).
- ³⁷*Ultrafast Infrared and Raman Spectroscopy*, edited by M. D. Fayer (Marcel Dekker, New York, 2001).
- ³⁸*Chem. Phys.* **266** (2–3), (2001), special issue on optical and infrared multidimensional spectroscopies.
- ³⁹M. Bonn, Ch. Hess, J. H. Miners, H. J. Bakker, T. F. Heinz, and M. Cho, *Phys. Rev. Lett.* **86**, 1566 (2001).
- ⁴⁰G. D. Mahan and A. A. Lucas, *J. Chem. Phys.* **68**, 1344 (1978).
- ⁴¹M. Scheffler, *Surf. Sci.* **81**, 562 (1979).
- ⁴²H. Pfnür, D. Menzel, F. M. Hoffmann, A. Ortega, and A. M. Bradshaw, *Surf. Sci.* **93**, 431 (1980).
- ⁴³H. Pfnür and H. J. Heier, *Ber. Bunsenges. Phys. Chem.* **90**, 272 (1986).
- ⁴⁴S. Funk, M. Bonn, D. N. Denzler, Ch. Hess, M. Wolf, and G. Ertl, *J. Chem. Phys.* **112**, 9888 (2000).
- ⁴⁵B. N. J. Persson and R. Ryberg, *Phys. Rev. B* **24**, 6954 (1981).
- ⁴⁶B. N. J. Persson, F. M. Hoffmann, and R. Ryberg, *Phys. Rev. B* **34**, 2266 (1986).
- ⁴⁷P. Jakob and D. Menzel, *Surf. Sci.* **201**, 503 (1988).
- ⁴⁸P. Jakob, *Phys. Rev. Lett.* **77**, 4229 (1996).
- ⁴⁹P. Jakob and B. N. J. Persson, *Phys. Rev. B* **56**, 10 644 (1997).
- ⁵⁰P. Jakob (private communication).
- ⁵¹Ch. Hess, M. Bonn, S. Funk, and M. Wolf, *Chem. Phys. Lett.* **325**, 139 (2000).
- ⁵²P. Jakob and B. N. J. Persson, *J. Chem. Phys.* **109**, 8641 (1998).